

Article

Relative Pollen Productivity Estimates for Major Plant Taxa in Middle Subtropical China

Qiuchi Wan ¹, Kangyou Huang ^{1,2,*}, Cong Chen ¹, Yongjie Tang ¹, Xiao Zhang ¹, Zhong Zhang ³ and Zhuo Zheng ^{1,2}

- ¹ Guangdong Provincial Key Laboratory of Geodynamics and Geohazards, School of Earth Sciences and Engineering, Sun Yat-sen University, Zhuhai 519082, China; wanqch@mail3.sysu.edu.cn (Q.W.); chenc66@mail.sysu.edu.cn (C.C.); tangyj55@mail.sysu.edu.cn (Y.T.); zhangx249@mail2.sysu.edu.cn (X.Z.); eeszzhuo@mail.sysu.edu.cn (Z.Z.)
- ² Southern Marine Science and Engineering Guangdong Laboratory (Zhuhai), Zhuhai 519082, China
- ³ Changguling Forest Farm, Jingtangshan National Nature Reserve, Jingtangshan 343600, China; syzz2010@126.com
- * Correspondence: hkangy@mail.sysu.edu.cn

Abstract: Relative pollen productivity (RPP) is a key parameter for quantitative reconstruction of past vegetation cover. However, RPP estimates are rarely obtained in the subtropical and tropical regions. In this study, the extended *R*-value (ERV) model was used to estimate RPP for major plant taxa in the evergreen broadleaved and mixed forests in middle subtropical China based on soil samples and vegetation data from 23 sites. The best result was obtained with the combinations of ERV sub-model 3 and Prentice's or 1/d vegetation distance-weighting method. The relevant source area of pollen (RSAP) of the soil samples was estimated to be ca. 500 m. RPP on the basis of ERV sub-model 3 and Prentice's model was obtained for seven taxa and the ranking is as follows: *Castanopsis* (1 ± 0), *Ilex* (0.352 ± 0.031), *Mallotus* (0.221 ± 0.028), *Liquidambar* (0.115 ± 0.007), *Cyclobalanopsis* (0.107 ± 0.006), *Camelia* (0.033 ± 0.001), *Symplocos* (0.010 ± 0.002). RPPs for *Cyclobalanopsis*, *Camelia*, *Ilex*, and *Symplocos* which are dominant elements in the subtropical evergreen broadleaved forests were first obtained. Our result demonstrates a significant effect of pollen dispersal models on the estimates of RPPs. The RPPs obtained in this study provide an important basis for quantitative vegetation reconstruction in the subtropical region of China.

Keywords: evergreen broadleaved forest; extended *R*-value model; pollen-vegetation relationship



Citation: Wan, Q.; Huang, K.; Chen, C.; Tang, Y.; Zhang, X.; Zhang, Z.; Zheng, Z. Relative Pollen Productivity Estimates for Major Plant Taxa in Middle Subtropical China. *Land* **2023**, *12*, 1337. <https://doi.org/10.3390/land12071337>

Academic Editor: Benjamin Burkhard

Received: 15 May 2023

Revised: 24 June 2023

Accepted: 27 June 2023

Published: 3 July 2023



Copyright: © 2023 by the authors. Licensee MDPI, Basel, Switzerland. This article is an open access article distributed under the terms and conditions of the Creative Commons Attribution (CC BY) license (<https://creativecommons.org/licenses/by/4.0/>).

1. Introduction

The current state of the biosphere is not only affected by ongoing climate change but also by the history of (anthropogenic) land-cover change [1,2] and feedback between land-cover and the climate system [3]. Therefore, it is crucial to reconstruct past land-cover change and investigate its relationship with human activities and the climate to anticipate the impact of current and future anthropogenic climate change on the environment. Pollen analysis is one of the most important methods for past vegetation reconstruction. Several pollen-based methods have been developed including, e.g., modern analogue [4], and biomization [5]. The landscape reconstruction algorithm (LRA) is a theory-based approach to the quantitative reconstruction of land-cover changes. It includes two models, the REVEALS (Regional Estimates of VEgetation Abundance from Large Sites) model to estimate regional vegetation composition [6] and the LOVE (LOcal VEgetation Estimates) model to estimate local vegetation composition within the relevant source area of pollen (RASP) [7]. The LRA relies on one important parameter, relative pollen productivity (RPP), which can be estimated with the extended *R*-value (ERV) models [8–10]. The ERV models can reduce the effects of the non-linear nature of the pollen percentage-vegetation relationships and make it possible to objectively estimate pollen productivity. Considering that biases in

pollen production and dispersal for a taxon are the main factors controlling pollen representation of plant abundance, the ERV models have a major assumption on pollen dispersal that the wind above the vegetation canopy is the dominant agent for pollen transport. The RPP has now been estimated for a wide range of plants in temperate regions where wind pollination is more common than in the tropics [11–14]. This has aided large-scale quantitative estimates of Holocene land-cover changes which in turn provides important information to assess the interactions between land-cover changes and climate in the past (e.g., [15,16]). However, attempts to estimate RPPs in tropical and subtropical regions of the world are rare, including only several studies from China and South Africa [17–22]. The difficulty of such attempts includes a wide variety of pollen productivity and dispersal mechanisms of plant species in the tropics with extremely high biodiversity [17].

Here we represent RPP results from a middle subtropical region of China, which is dominated by zonal evergreen broadleaved forests [23]. The available RPPs obtained in subtropical China focused on deciduous species [20,21]. Thus, our study is an important supplement to the estimates of RPPs for major evergreen plant taxa. This would enable an accurate quantitative reconstruction of the evergreen plant covers in addition to the deciduous plant covers, contributing to a comprehensive understanding of the past vegetation succession in subtropical China which is important for the study of the origin of human rice agriculture and land-cover-human-climate interactions. By comparing the results based on several combinations of models, we also highlight the impact of pollen dispersal models on the estimates of RPPs. In view of a majority of studies relying on Prentice's model to estimate RPPs, we suggest validating the different RPP datasets produced with different dispersal models to obtain the most reliable estimates.

2. Study Area

Our study area is located within the Jinggangshan National Natural Reserve (Figure 1). The Jinggangshan Mountain region belongs to the middle subtropical climatic zone. The regional mean annual temperature is approximately 14 °C, and the mean annual precipitation is approximately 1800 mm [24]. The zonal vegetation in the Jinggangshan Mountains is a subtropical evergreen broadleaved forest. The vegetation composition in altitude is as follows [23]:

- (1) Evergreen broadleaved forest (<1000 m) dominated by *Castanopsis sclerophylla* (Lindl. et Paxton) Schottky, *Castanopsis concinna* (Champ. ex Benth.) A. DC., *Castanopsis fabri* Hance, *Castanopsis tibetana* Hance, *Machilus thunbergii* Sieb. et Zucc., *Phoebe humanensis* Hand.-Mazz., and *Elacocarpus japonicus* Sieb. et Zucc.
- (2) Mixed evergreen and broadleaved forest (1000–1400 m) composed of deciduous elements including *Castanopsis eyrei* (Champ. ex Benth.) Tutch., *Schima superba* Gardn. et Champ., and *Fagus lucida* Rehd. et Wils.
- (3) Shrub-meadow (>1400 m) on the mountain summits dominated by *Rhododendron simiarum* Hance, *Pieris formosa* (Wall.) D. Don, and *Enkianthus quinqueflorus* Lour.

Due to human disturbance, the present-day vegetation in the mountainside is composed of many secondary forest tree species such as *Pinus massoniana* Lamb., as well as *Phyllostachys edulis* (Carrière) J. Houz. (bamboo) [25]. The lowlands are covered largely by rice paddy.

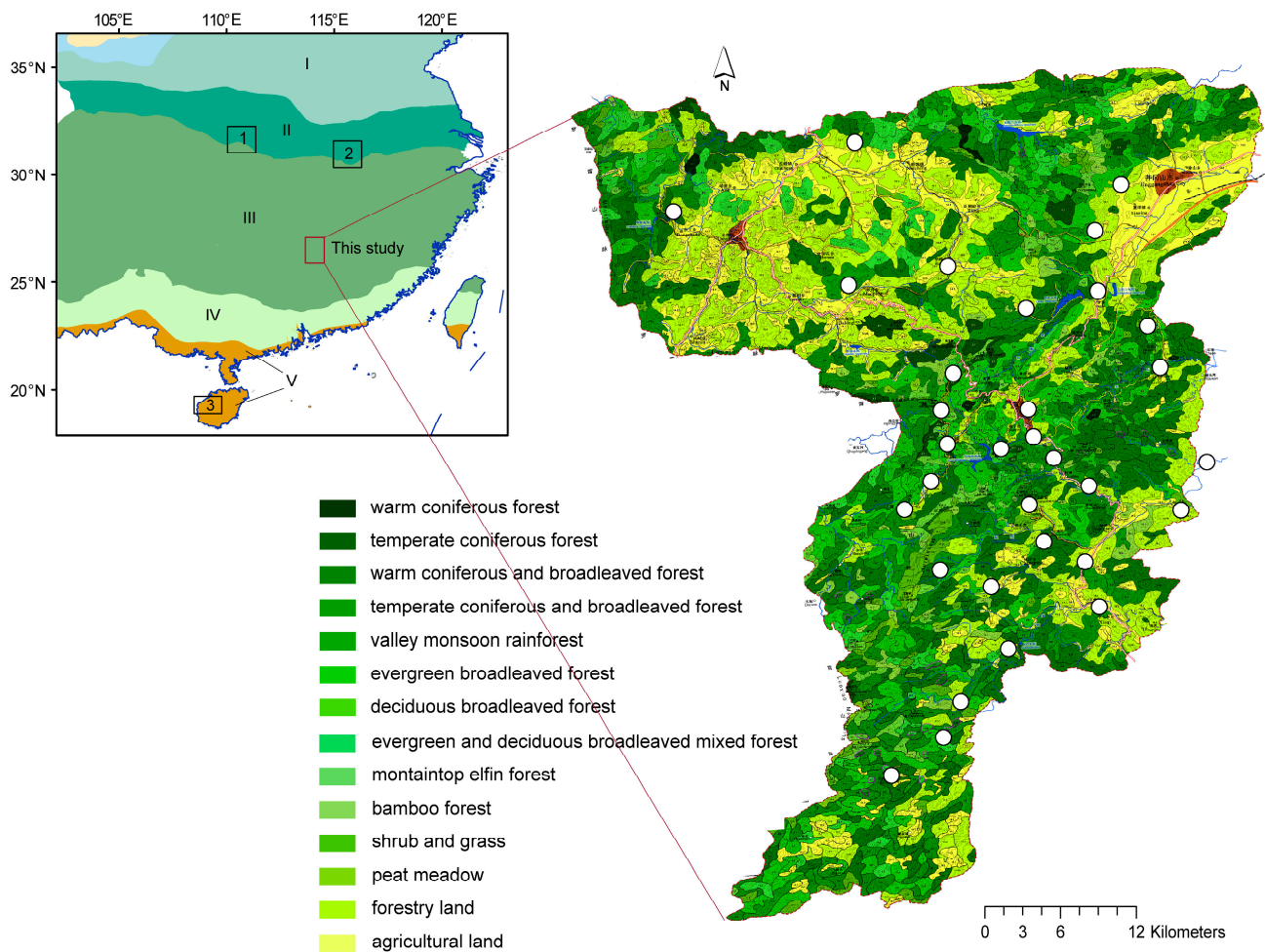


Figure 1. Land cover map of the study area (modified from [26]) and the distribution of the 32 studied modern sites (white dots). Other RPP studies from subtropical China are also shown in the inset: 1, Daba Mountains [21]; 2, Ta-pieh Mountains [20]; 3, Hainan cultural landscape [22]. The vegetation zones in the inset are illustrated by different colors and numbers: I, temperate deciduous forest zone; II, northern subtropical evergreen broadleaved forest zone (EVBF); III, middle EVBF; IV, southern EVBF; V, tropical seasonal rainforest zone.

3. Materials and Methods

3.1. Field Work

The field work was undertaken in August 2019 within a 50 km × 50 km area. A total of 32 sites were randomly selected with a distance of at least 3000 m between them to avoid auto-correlation (Figure 1). Next, 32 surface soil samples were collected from the top ~2 cm of the soil layer and consisted of several random sub-samples within an area of a 0.5 m radius at each of the sampling points.

Following the standard protocol of [27], we conducted a vegetation survey within a 100 m radius of the sampling points for further RPP estimates using the ERV model. The major vegetation communities recognized in the field are listed in Table 1.

Table 1. Location of the 32 studied sites and the major vegetation communities surveyed in the field within a 100 m radius area of the sampling sites.

Site	Latitude (°)	Longitude (°)	Elevation (m)	Major Vegetation Communities within 100 m
5	114.24	26.74	314	Woodland of <i>Cunninghamia R. Br. ex A. Rich.</i> and <i>Cryptomeria D. Don</i> ; Bamboo
6	114.18	26.47	520	Woodland of <i>Cyclobalanopsis Oerst.</i> and <i>Castanopsis Spach</i> ; crop field
14	114.12	26.35	441	Woodland of <i>Castanopsis Spach</i> and <i>Cunninghamia</i> ; Bamboo
18	114.11	26.32	480	Woodland of <i>Castanopsis</i> and <i>Castanea Mill.</i>
22	114.16	26.39	322	Woodland of <i>Castanopsis</i> , <i>Manglietia Blume</i> , and <i>Sterculia L.</i> ; Woodland of <i>Cunninghamia</i> ; Bamboo
27	114.11	26.68	320	Woodland of <i>Liquidambar L.</i> , <i>Camellia L.</i> , and <i>Schima Reinw. ex Blume</i> ; Bamboo; crop field
32	114.29	26.49	275	Woodland of <i>Cyclobalanopsis</i> , <i>Sassafras J. Presl</i> , and <i>Machilus Nees</i> ; crop field
33	114.22	26.71	380	Woodland of <i>Sapium Jacq.</i> , <i>Fissistigma Griff.</i> , <i>Eurya Thunb.</i> , and Myrtaceae Juss.; woodland of <i>Pinus L.</i> ; Bamboo
52	114.03	26.67	340	Woodland of <i>Machilus</i> , <i>Eurya</i> , and <i>Cinnamomum verum</i> ; Bamboo; crop field
222	114.19	26.53	524	Woodland of <i>Castanopsis</i> , <i>Exbucklandia R. W. Brown</i> , and <i>Garcinia L.</i>
223	114.17	26.65	642	Woodland of <i>Fagus L.</i> and <i>Castanopsis</i> ; crop field
DSC	113.9	26.72	240	Woodland of <i>Cyclobalanopsis</i> , <i>Schima</i> , and <i>Taiwania Hayata</i> ; woodland of <i>Camellia</i> ; crop field
GCZ	114.04	26.77	221	Woodland of <i>Pinus</i> and <i>Cunninghamia</i> ; Bamboo; crop field
N1	114.11	26.6	1300	Woodland of <i>Daphniphyllum Bl.</i> ; woodland of <i>Cryptomeria D. Don</i> ; woodland of <i>Castanopsis</i>
N2	114.1	26.57	1330	Woodland of <i>Eurya</i> and <i>Acer L.</i> ; woodland of <i>Cryptomeria</i>
N3	114.11	26.54	1180	Woodland of <i>Machilus</i> , <i>Pinus</i> , <i>Castanopsis</i> , and <i>Schima</i> ; Bamboo
S01	114.31	26.53	253	Woodland of <i>Castanopsis</i> , <i>Schima</i> , and <i>Cunninghamia</i> ; crop field
S05	114.22	26.51	377	Woodland of <i>Castanopsis</i> and <i>Distylium Siebold and Zucc.</i> ; Bamboo; crop field
S15	114.17	26.5	829	Woodland of <i>Castanopsis</i> , <i>Cunninghamia</i> , and <i>Cyclobalanopsis</i> ; woodland of <i>Cunninghamia</i>
S20	114.17	26.55	594	Woodland of <i>Castanopsis</i>
W1	114.26	26.63	690	Woodland of <i>Castanopsis</i> , <i>Machilus</i> , and <i>Eurya</i>
W10	114.1	26.52	910	Woodland of <i>Castanopsis</i> , <i>Liquidambar</i> , <i>Cyclobalanopsis</i> , and <i>Machilus</i> ; Bamboo; woodland of <i>Pinus</i> ; crop field; woodland of <i>Cryptomeria</i>
W11	114.15	26.54	880	Woodland of <i>Cunninghamia</i> , <i>Cyclobalanopsis</i> , <i>Castanopsis</i>
W2	114.27	26.6	370	Woodland of <i>Schima</i> , <i>Symplocos</i> , and <i>Castanopsis</i> ; woodland of <i>Cunninghamia</i> ; Bamboo; crop field
W3	114.22	26.66	370	Woodland of <i>Castanopsis</i> and <i>Ardisia Sw.</i> ; woodland of <i>Cunninghamia</i> ; Bamboo; crop field
W4	114.17	26.57	750	Woodland of <i>Castanopsis</i> and <i>Schima</i> ; woodland of <i>Camellia</i>
W5	114.22	26.42	269	Woodland of <i>Castanopsis</i> and <i>Lophatherum Brongn.</i> ; woodland of <i>Cunninghamia</i> ; Bamboo; crop field
W6	114.14	26.44	776	Woodland of <i>Castanopsis</i> and <i>Michelia L.</i> ; Bamboo; crop field
W7	114.1	26.45	310	Woodland of <i>Liquidambar</i> and <i>Cyclobalanopsis</i> ; Bamboo; grassland
W8	114.21	26.46	340	Woodland of <i>Castanopsis</i> and <i>Schima</i> ; Bamboo; crop field
W9	114.08	26.5	1200	Woodland of <i>Castanopsis</i> and <i>Cunninghamia</i> ; Bamboo
Y1	114.07	26.29	1076	Woodland of <i>Acer</i> and <i>Rhododendron L.</i> ; crop field

3.2. Pollen Analysis

Pollen samples were processed following the standard procedures of [28]. One piece of marker tablet with exotic *Lycopodium* (27,560 spores per piece) was added to each sample for calculation of pollen concentrations. Samples were treated with 10% HCl for carbonate removal and 10% KOH for humic acid removal. Coarse soil particles and other plant fragments were removed with a 0.125 mm mesh sieve. Heavy ZnBr₂ liquid, 1.9–2.0 g/cm³, was used for gravity separation and the process was undertaken twice. Residues were mounted in glycerol on glass slides and sealed with Canada Balsam. Pollen grains were identified under 400× magnification with a Nikon and ZEISS light microscope and under 1000× magnification for more detailed examination. A minimum of 500 pollen grains were counted in each sample. Several references were used for pollen identification including

vegetation [8]. The ERV sub-models 1 and 2 assume and estimate a species-specific constant background in pollen proportion and in the proportion of pollen loading to total plant abundance of all the taxa involved, respectively [8]. In addition, the relative cover (in percentage or proportion) of each plant taxon (harmonized with a pollen morphological type) is used in both sub-models. The ERV sub-model 3 does not have any additional assumption on the background pollen and utilizes the absolute cover of each plant taxon (in m^2/m^2). The three sub-models generally provide similar results. However, many cases have shown that one sub-model is more appropriate than the others, e.g., [34,35]. It might reflect that the vegetation data violate the assumption of the sub-models. In theory, pollen loading is linearly related to the distance-weighted plant abundance for each taxon [10]. Several methods have been developed to calculate the distance-weighted plant abundance, for example, the inverse distance ($1/d$), Prentice's model [36], and the Lagrangian stochastic dispersal model (LSM) [37]. The LSM was suggested to be more powerful for the description of pollen dispersal when entomophilous plants dominate the vegetation [38]. However, it was not the case when the LSM was applied in the tropical Hainan Island [22]. Generally, different combinations of ERV sub-models and distance-weighting methods are used and their results are compared in one study to obtain the most suitable combination and most reliable estimates of the RPP dataset and RSAP.

For running the ERV model, plant taxa were first harmonized with pollen types (Table 2). The plant/pollen taxa were then selected for RPP estimates. The basic criterion for the selection is that the vegetation and pollen data exhibit a good spread of values from low to high in one taxon. A reference taxon ($\text{RPP} = 1$) was used to calculate the RPPs of all other taxa. Poaceae is commonly used as a reference taxon as it occurs frequently in the vegetation and pollen in temperate regions (e.g., [11,33,39]). In our study region, Poaceae occurs in different forms and is not appropriate for ERV modeling (see discussion). We finally chose *Castanopsis* as the reference taxon because it is abundant in both pollen and vegetation data.

Three datasets are required for ERV modeling, i.e., pollen counts, fall speed of pollen, and vegetation data. Apart from these, several parameters were set as follows: basin size (0.5 m), and wind speed (3 m/s). The ERV model was first run with the selected taxa (Table 2) and 32 sites. The ERV-adjusted pollen values and distance-weighted vegetation cover were plotted to select the taxa with the most linear pollen-vegetation relationships and remove some outlier sites. This procedure was repeated several times with a reduced number in taxa and sites (i.e., seven taxa and 23 sites in the final run) until the log-likelihood curve reached the theoretically best shape, i.e., increased with distance and reached an asymptote within the area of vegetation survey (1500 m).

4. Results and Discussion

4.1. Modern Vegetation and Surface Pollen Assemblages

The 32 sites are classified as evergreen woodland (EW) and mixed woodland (MW) (Figure 2), based on surveyed plant taxa from 93 families and 219 genera. The principal arboreal taxa in EW are *Castanopsis*, *Cyclobalanopsis*, Lauraceae Juss. (comprising mainly *Machilus*, *Cinnamomum*, and *Sassafras*), and Theaceae Mirb. (e.g., *Eurya*, *Schima*, and *Camellia*). The vegetation in MW comprises a mix of evergreen taxa similar to EW and coniferous and deciduous broadleaved trees and shrubs, such as Taxodiaceae Warming (comprising mainly *Cunninghamia*), *Pinus*, Liquidambar, Ericaceae Juss. (e.g., *Rhododendron*), *Acer*, and *Fagus*. Bamboo (e.g., *Phyllostachys* Siebold and Zucc., *Indocalamus* Nakai) also frequently occurs in these sites with high coverage. Herbs including mainly Poaceae are not abundant in our studied sites.

A total of 83 pollen types were identified at the genus-to-family levels in the 32 surface soil samples. Dominant pollen taxa in EW sites include arboreal types *Castanopsis*-*Lithocarpus*, *Cyclobalanopsis*, *Camelia*, *Pinus*, *Ilex*, *Eurya*, and non-arboreal Poaceae (Figure 2). Pollen assemblages of MW sites are similar to EW sites with differences in higher percentages of *Pinus* and Liquidambar.

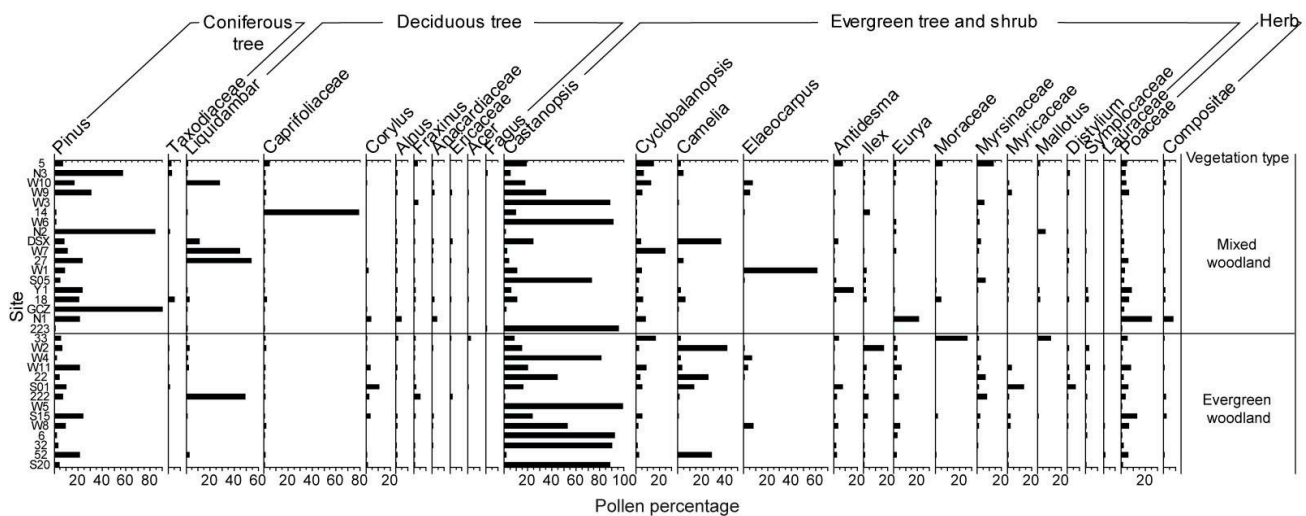


Figure 2. Pollen percentage diagram of the major pollen taxa found in the 32 surface soil samples.

Comparing percentages of vegetation cover and pollen, most evergreen broadleaved taxa have good pollen representation (e.g., *Castanopsis*, *Cyclobalanopsis*, *Camellia*, and *Ilex*); whereas, few or no pollen were found in the Lauraceae community. Deciduous taxa tend to be under-represented in surface pollen (*Liquidambar* as an exception). The coniferous tree *Pinus* is over-represented in surface pollen while *Taxodiaceae* is significantly under-represented. Considering this, seven taxa (Table 1) that have good spread values in both vegetation cover and pollen were selected for the final ERV analysis: *Castanopsis*, *Liquidambar*, *Cyclobalanopsis*, *Camellia*, *Ilex*, *Mallotus*, and *Symplocos*.

4.2. Relevant Source Area of Pollen and Affecting Factors

Figure 3 shows the log-likelihood curves of the nine combinations of ERV sub-models and distance-weighting models. For a given distance-weighting model, ERV sub-model 1 tends to have the poorest performance in terms of the lowest log-likelihood values among the three ERV sub-models and the increasing trend of the log-likelihood curve in comparison with an expected pattern, i.e., gradually increasing to reach an asymptote. The poor performance of ERV sub-model 1 is expected because ERV sub-model 1 assumes that the background pollen loading is a constant proportion of the total pollen loading [8]. Such assumption can be easily violated by variations in among-site vegetation composition and among-taxon pollen productivity as commonly observed in previous studies (e.g., [40]). ERV sub-models 2 and 3 have similar equations to linearize the pollen-vegetation relationship, but they differ in the way of expressing the vegetation (as percentages and projection area per unit area utilized by ERV sub-models 2 and 3, respectively) [10]. When non-pollen-producing areas (rocks, roads, water, etc.) are not included in the analysis, the input vegetation data are the same in both sub-models. As our study area is a fine mosaic of forests and croplands, there is a negligible proportion of non-pollen-producing areas. This could explain the similar log-likelihood values of ERV sub-models 2 and 3 with the latter being closer to an expected pattern of the log-likelihood curve. The combinations of ERV sub-model 3 with Prentice's and $1/d$ vegetation distance-weighting methods show very similar values and trends of the log-likelihood. The combination of ERV sub-model 3 and LSM distance-weighting produces the highest log-likelihood values with a high variation. In general, ERV sub-model 3 with Prentice's or $1/d$ vegetation distance-weighting method produces the most expected log-likelihood curve (i.e., gradually increasing to reach an asymptote), and thus is considered the best result in this study.

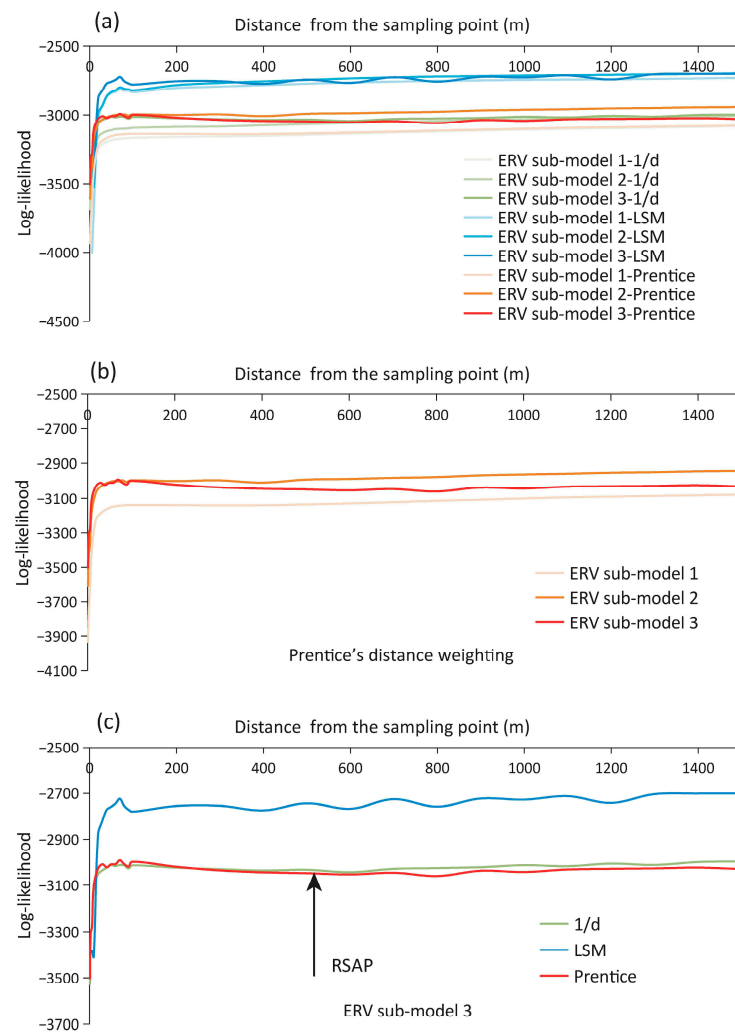


Figure 3. Plots of the log-likelihood values with distance for nine combinations of three ERV sub-models and three distance-weighting methods (Prentice's model, inverse distance ($1/d$), and Lagrangian Stochastic Model (LSM)), using pollen data from modern surface soil samples at 23 random sites and related vegetation data within 1500 m radius around each sample. (a) nine combinations of the models; (b) a combination of Prentice's distance weighting method and three ERV sub-models; (c) a combination of ERV sub-model 3 and three distance-weighting methods.

For the best combination of models (ERV sub-model 3 with Prentice's or $1/d$ vegetation distance weighting method), the log-likelihood curve reaches an asymptote with relatively constant values beyond ca. 500 m (Figure 3c). Thus, the estimated RSAP is 500 m. This value is slightly higher than other values estimated in a subtropical forest landscape in China (e.g., 340 m in Ta-pieh Mountains [20], 360 m in Daba Mountains [21]), but the same as the value estimated in the tropical Hainan Forest landscape (i.e., 500 m [22]). RSAP might be influenced by many factors such as size and type of sediment basin and vegetation structure (e.g., patch size, the spatial distribution of patches, and plant taxa in the landscape). Previous studies have demonstrated that when the basin size was constant, the size of the vegetation patch would have a very significant effect on the RSAP [33]. In this study, the land-cover maps were created based on visual interpretation instead of the typically used supervision and non-supervision classification methods. As a result, the resolution of our land-cover maps is lower compared to previous studies. Thus, we expected a higher RSAP than previous studies because of the large vegetation patches being extracted. In addition, the pollen samples were collected from surface soil in both Hainan [22] and this study, while moss polster samples were studied in the two mentioned subtropical works [20,21].

It is suggested that soil pollen assemblages contain a larger background pollen component than the moss assemblages [41]. This could result in a higher RSAP when estimated with soil pollen samples compared to moss samples. Therefore, the higher RSAP estimate in this study might be influenced by both the resolution of the land cover maps and the basin type. It would be worth testing the contributions of the two factors to the estimation of RSAP.

4.3. Pollen-Vegetation Relationships

The scatter plots of ERV-adjusted pollen and vegetation values using ERV sub-model 3 and Prentice's vegetation distance-weighting method at the RSAP of 500 m are shown in Figure 4. The pollen-vegetation relationship of *Castanopsis* shows a very good linear trend. For *Cyclobalanopsis*, *Liquidambar*, and *Ilex*, the spread of pollen and vegetation values are more or less close to a linear trend. *Camelia* and *Symplocos* exhibit a large spread of values with high plant cover that may correspond to low pollen value while low plant cover corresponds to high pollen value. There is a single high value in the pollen and vegetation data of *Mallotus*. In most cases, extremely low values of plant covers correspond to a range of pollen loading. Similar findings were obtained in a tropical study which is ascribed to entomophily for *Mallotus* [22]. This could also explain the poor relationships between pollen and vegetation observed in *Camelia* and *Symplocos* in this study. ERV model assumes pollen anemophily [8–10]. The violation of the basic assumption of the model already indicates that it is difficult to perform pollen-vegetation calibration for such taxa. Thus, the resulting RPPs for these taxa should be treated and evaluated with care.

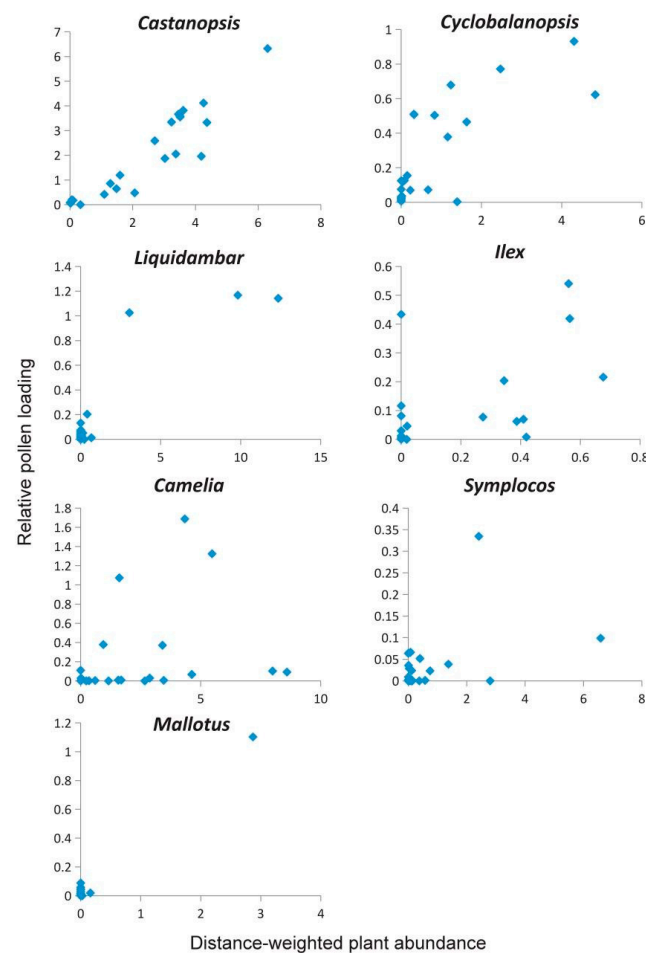


Figure 4. Scatter plots of the pollen-vegetation relationships at the distance of the relevant source area of pollen (RSAP = 500 m) as estimated using the ERV sub-model 3 and Prentice's vegetation distance-weighting method.

4.4. Relative Pollen Productivity Estimates

We estimated RPPs for seven plant/pollen taxa, among which the RPPs for four taxa were first estimated, i.e., *Cyclobalanopsis*, *Camelia*, *Ilex*, and *Symplocos*. The nine combinations of the models yield some variation in the estimated RPPs which differ mainly from the applied pollen dispersal models (Table 3). Previous studies have also found a larger impact of the distance-weighting method on the estimated RPPs than the selection of ERV sub-models (e.g., [12]). In this study, the values (using *Castanopsis* as the reference) produced with Prentice's model are consistently lower than those produced with 1/d and LSM model irrespective of the plant taxon and ERV models used. The 1/d and LSM models tend to produce similar values of RPPs. Similar result between the 1/d and LSM model is reasonable because the impact of taxon-specific fall speed is nearly negligible for fall speeds smaller than 0.04 m/s in the LSM [37] and 1/d does not consider the inter-taxonomic differences in pollen dispersal. However, the fall speed of pollen has a much larger impact on Prentice's model which uses a Gaussian plume diffusion model (GPM) which was suggested to predict higher RPPs for taxa with large pollen with high fall speed [12,42,43]. In the case of this study, *Castanopsis* has the lowest FSP (0.0034 m/s). The resulting RPPs with the GPM (i.e., higher RPP for *Castanopsis* and lower for the other taxa compared to the result of 1/d) do not follow but rather contradict the suggested trend, i.e., higher RPPs for large pollen while lower RPPs for small pollen [42]. A similar result in this study was also obtained in other studies [14,38]. For example, in the study of [14], the 1/d method always produced lower RPPs for *Castanea* (a sister lineage to *Castanopsis* and usually used for comparison) than with Prentice's distance-weighting method. The disagreement between the studies regarding the relationships between pollen size and RPP might be largely due to the Gaussian formulation-based calculation of the distance-weighted plant abundance (DWPA) in Prentice's model. Such calculation can lead to a lower DWPA (thus a higher RPP) for a taxon with both too high and too low fall speed.

Table 3. Relative pollen productivity (RPP) with standard error for eight taxa estimated with the ERV sub-models and three vegetation distance-weighting methods, i.e., Prentice's taxon-specific model, the inverse distance (1/d), and the Lagrangian stochastic model (LSM).

Taxa	ERV 1 Prentice	ERV 2 Prentice	ERV 3 Prentice	ERV 1 1/d	ERV 2 1/d	ERV 3 1/d	ERV 1 LSM	ERV2 LSM	ERV 3 LSM
<i>Castanopsis</i>	1 ± 0	1 ± 0	1 ± 0	1 ± 0	1 ± 0	1 ± 0	1 ± 0	1 ± 0	1 ± 0
<i>Ilex</i>	0.354 ± 0.03	0.324 ± 0.028	0.352 ± 0.031	0.936 ± 0.079	0.827 ± 0.071	0.861 ± 0.076	1.204 ± 0.104	1.096 ± 0.098	1.159 ± 0.101
<i>Mallotus</i>	0.558 ± 0.088	0.532 ± 0.085	0.221 ± 0.028	1.166 ± 0.201	0.762 ± 0.109	0.615 ± 0.092	1.377 ± 0.228	1.104 ± 0.191	1.578 ± 0.283
<i>Liquidambar</i>	0.116 ± 0.006	0.106 ± 0.006	0.115 ± 0.007	0.421 ± 0.023	0.388 ± 0.022	0.398 ± 0.023	0.855 ± 0.042	0.823 ± 0.044	0.815 ± 0.042
<i>Cyclobalanopsis</i>	0.124 ± 0.007	0.109 ± 0.006	0.107 ± 0.006	0.263 ± 0.014	0.243 ± 0.014	0.227 ± 0.013	0.843 ± 0.046	0.797 ± 0.045	0.7 ± 0.039
<i>Camelia</i>	0.034 ± 0.001	0.032 ± 0.001	0.033 ± 0.001	0.12 ± 0.005	0.114 ± 0.005	0.113 ± 0.005	0.214 ± 0.009	0.207 ± 0.008	0.205 ± 0.008
<i>Symplocos</i>	0.011 ± 0.002	0.009 ± 0.002	0.01 ± 0.002	0.044 ± 0.006	0.038 ± 0.006	0.04 ± 0.006	0.052 ± 0.008	0.043 ± 0.008	0.036 ± 0.006

By observing the large difference in the estimated RPPs using different distance-weighting methods, a majority of studies preferred to use the GPM for RPP calculation [12]. Others demonstrated that the LSM is more realistic [38,42]. In this study, Prentice's model apparently increases the RPP for *Castanopsis* and decreases the RPPs for the others compared to the other distance-weighting methods. Further study is needed to evaluate the appropriateness of these models.

Many studies use Poaceae as a reference taxon to estimate RPPs because it is one of the most common pollen types in the open and semi-open vegetation in the temperate zone. However, in the subtropical zone of China, Poaceae mainly occurs as bamboo in the mountainside. Different from other Poaceae herbs, most species of bamboo bloom only once in their lifetime and were demonstrated to have a significant effect on the estimated RPPs [20]. Our test runs with Poaceae included illustrate a similar result. Therefore, Poaceae was not included in our RPP estimates. *Pinus* was neither included in this study although it has large spread values in both vegetation and pollen data. The reason is that the average plant abundance of *Pinus* among sites shows a continuously increasing trend as distance increases, which violates the assumption of the ERV model of stationary vegetation (results not shown) [10].

There are two available subtropical works, one tropical work, and one synthesized temperate dataset from China that can be compared with the RPPs obtained in this study. All RPPs were converted to values relative to *Castanopsis/Castanea* (Table 4). Overall, our estimated RPPs based on ERV sub-model 3 and Prentice's or 1/d vegetation distance-weighting method are generally comparable with other published values obtained in China. The RPP estimates for *Liquidambar* and *Cyclobalanopsis* produced with 1/d distance-weighting are more similar to previous studies than Prentice's model whereas the RPP for *Mallotus* estimated with Prentice's model is closer to the one published value than the 1/d method. Given that few RPP estimates are available for comparison, a further validation of these values using a REVEALS model-based method (see the application of this method in [44]) would enable a more meaningful comparison between studies.

Table 4. Comparison of relative pollen productivity (RPP) estimates between this study and other values obtained in China.

Study Area	Jinggangshan Mountains	Temperate China	Ta-Pieh Mountains	Daba Mountains	Hainan Cultural Landscapes
Model combinations	ERV3_Prentice/1/d	Alt-1	ERV1_Prentice	ERV2_Prentice	ERV2_Prentice
<i>Castanopsis/Castanea</i>	1	1	1	1	1
<i>Liquidambar</i>	0.12/0.40		0.28		
<i>Cyclobalanopsis/Quercus</i>	0.11/0.23	0.38	1.89	2.70	
<i>Mallotus</i>	0.22/0.62				0.11
Reference	This study	Li et al. (2018) [39]	Chen et al. (2019) [20]	Jiang et al. (2020) [21]	Wan et al. (2020) [22]

The RPPs from other studies were all converted to values relative to *Castanopsis/Castanea*.

5. Conclusions

A new RPP dataset from middle subtropical China was obtained which adds the first RPPs from several dominant elements in the evergreen broadleaved forest including *Cyclobalanopsis*, *Camelia*, *Ilex*, and *Symplocos*. The most important finding is that the application of different pollen dispersal models results in large different RPPs. Prentice's model uses a Gaussian plume diffusion model apparently increases the RPP for *Castanopsis* with a very low fall speed as compared to 1/d and the LSM model. This result seems to contradict previous studies showing that the GPM would overestimate the RPPs for pollen with a high fall speed while underestimating for pollen with a low fall speed. Indeed, the Gaussian formulation-based Prentice's model can lead to lower DWPA (thus a higher RPP) for a taxon with both too high and too low fall speed. By demonstrating the significant effect of pollen dispersal models on the RPP estimates and in view of a majority of studies relying on Prentice's model to estimate RPPs, we suggest validating the different RPP datasets produced with different dispersal models in a real case, e.g., comparing the observed vegetation with an RPP dataset and REVEALS model-based land cover reconstruction.

Author Contributions: Conceptualization, Q.W.; funding acquisition, Q.W., K.H. and Z.Z. (Zhuo Zheng); investigation, Q.W., K.H., X.Z., Z.Z. (Zhong Zhang) and Z.Z. (Zhuo Zheng); methodology, Q.W.; software, Q.W.; writing—original draft, Q.W.; writing—review and editing, Q.W., K.H., C.C., Y.T., X.Z. and Z.Z. (Zhuo Zheng). All authors have read and agreed to the published version of the manuscript.

Funding: This research was funded by the National Natural Science Foundation of China (grant numbers 42077414, 42072205, 41630753, and 41902186), the Innovation Group Project of Southern Marine Science and Engineering Guangdong Laboratory (Zhuhai) (grant number 311020002), and the Project of the Influence of Quaternary Glacial Cycle on Biodiversity in Nanling Mountains (grant Number 2021GJGY001). We also acknowledge the financial support from the Swedish Foundation for International Cooperation in Research and Higher Education (STINT), and the NSFC [grant number 41611130050] for a Sweden-China Exchange Grant 2016–2019 (PIs Marie-José Gaillard and Qinghai Xu). This study was undertaken as part of the Past Global Changes (PAGES) project and its working group LandCover6k, which in turn received support from the U.S. National Science Foundation and the Swiss Academy of Sciences.

Data Availability Statement: The data presented in this study are available on request from the corresponding author.

Acknowledgments: The authors would like to thank Zhen Li, Qiang Fan and Wenbo Liao for providing the vegetation survey data. We also thank all members of the palynology team at Sun Yat-sen University for their help with field work.

Conflicts of Interest: The authors declare no conflict of interest.

References

- Zheng, Z.; Ma, T.; Roberts, P.; Li, Z.; Yue, Y.; Peng, H.; Huang, K.; Han, Z.; Wan, Q.; Zhang, Y.; et al. Anthropogenic impacts on Late Holocene land-cover change and floristic biodiversity loss in tropical southeastern Asia. *Proc. Natl. Acad. Sci. USA* **2021**, *118*, e2022210118. [[CrossRef](#)] [[PubMed](#)]
- Ellis, E.C.; Gauthier, N.; Goldewijk, K.K.; Bird, R.B.; Boivin, N.; Díaz, S.; Fuller, D.Q.; Gill, J.L.; Kaplan, J.O.; Kingston, N.; et al. People have shaped most of terrestrial nature for at least 12,000 years. *Proc. Natl. Acad. Sci. USA* **2021**, *118*, e2023483118. [[CrossRef](#)] [[PubMed](#)]
- Harrison, S.P.; Stocker, B.D.; Klein Goldewijk, K.; Kaplan, J.O.; Braconnot, P. Do we need to include anthropogenic land-use and land-cover changes in paleoclimate simulations? *Past Glob. Chang. Mag.* **2018**, *26*, 4–5. [[CrossRef](#)]
- Overpeck, J.T.; Webb, T., III; Prentice, I.C. Quantitative interpretation of fossil pollen spectra: Dissimilarity coefficients and the method of modern analogs. *Quat. Res.* **1985**, *23*, 87–108. [[CrossRef](#)]
- Prentice, I.C.; Guiot, J.; Huntley, B.; Jolly, D.; Cheddadi, R. Reconstructing biomes from palaeoecological data: A general method and its application to European pollen data at 0 and 6 ka. *Clim. Dyn.* **1996**, *12*, 185–194. [[CrossRef](#)]
- Sugita, S. Theory of quantitative reconstruction of vegetation I: Pollen from large sites REVEALS regional vegetation composition. *Holocene* **2007**, *17*, 229–241. [[CrossRef](#)]
- Sugita, S. Theory of quantitative reconstruction of vegetation II: All you need is LOVE. *Holocene* **2007**, *17*, 243–257. [[CrossRef](#)]
- Prentice, I.C.; Parsons, R.W. Maximum likelihood linear calibration of pollen spectra in terms of forest composition. *Biometrics* **1983**, *39*, 1051–1057. [[CrossRef](#)]
- Sugita, S. A model of pollen source area for an entire lake surface. *Quat. Res.* **1993**, *39*, 239–244. [[CrossRef](#)]
- Sugita, S. Pollen representation of vegetation in Quaternary sediments: Theory and method in patchy vegetation. *J. Ecol.* **1994**, *82*, 881–897. [[CrossRef](#)]
- Broström, A.; Nielsen, A.B.; Gaillard, M.-J.; Hjelle, K.; Mazier, F.; Binney, H.; Bunting, J.; Fyfe, R.; Meltsov, V.; Poska, A.; et al. Pollen productivity estimates of key European plant taxa for quantitative reconstruction of past vegetation: A review. *Veg. Hist. Archaeobotany* **2008**, *17*, 461–478. [[CrossRef](#)]
- Poska, A.; Meltsov, V.; Sugita, S.; Vassiljev, J. Relative pollen productivity estimates of major anemophilous taxa and relevant source area of pollen in a cultural landscape of the hemi-boreal forest zone (Estonia). *Rev. Palaeobot. Palynol.* **2011**, *167*, 30–39. [[CrossRef](#)]
- Xu, Q.; Cao, X.; Tian, F.; Zhang, S.; Li, Y.; Li, M.; Li, J.; Liu, Y.; Liang, J. Relative pollen productivities of typical steppe species in northern China and their potential in past vegetation reconstruction. *Sci. China Earth Sci.* **2013**, *57*, 1254–1266. [[CrossRef](#)]
- Li, F.; Gaillard, M.-J.; Sugita, S.; Mazier, F.; Xu, Q.; Zhou, Z.; Zhang, Y.; Li, Y.; Laffly, D. Relative pollen productivity estimates for major plant taxa of cultural landscapes in central eastern China. *Veg. Hist. Archaeobotany* **2017**, *26*, 587–605. [[CrossRef](#)]
- Kleinen, T.; Tarasov, P.; Brovkin, V.; Andreev, A.; Stebich, M. Comparison of modeled and reconstructed changes in forest cover through the past 8000 years. *Holocene* **2011**, *21*, 723–734. [[CrossRef](#)]
- Kuosmanen, N.; Marquer, L.; Tallavaara, M.; Molinari, C.; Zhang, Y.; Alenius, T.; Edinborough, K.; Pesonen, P.; Reitalu, T.; Renssen, H.; et al. The role of climate, forest fires and human population size in Holocene vegetation dynamics in Fennoscandia. *J. Veg. Sci.* **2018**, *29*, 382–392. [[CrossRef](#)]
- Gaillard, M.-J.; Githumbi, E.; Achoundong, G.; Lézine, A.-M.; Hély, C.; Lebamba, J.; Marquer, L.; Mazier, F.; Li, F.; Sugita, S. The Challenge of Pollen-Based Quantitative Reconstruction of Holocene Plant Cover in Tropical Regions: A Pilot Study in Cameroon. In *Quaternary Vegetation Dynamics, the African Pollen Database*; Runge, J., Gosling, W.D., Lézine, A.-M., Scott, L., Eds.; CRC Press: Boca Raton, FL, USA, 2021; pp. 183–206.
- Tabares, X.; Ratzmann, G.; Kruse, S.; Theuerkauf, M.; Mapani, B.; Herzsuh, U. Relative pollen productivity estimates of savanna taxa from southern Africa and their application to reconstruct shrub encroachment during the last century. *Holocene* **2021**, *31*, 1100–1111. [[CrossRef](#)]
- Duffin, K.I.; Bunting, M.J. Relative pollen productivity and fall speed estimates for southern African savanna taxa. *Veg. Hist. Archaeobotany* **2007**, *17*, 507–525. [[CrossRef](#)]
- Chen, H.; Xu, Q.; Zhang, S.; Sun, Y.; Wang, M.; Zhou, Z. Relative pollen productivity estimates of subtropical evergreen and deciduous broadleaved mixed forest in Ta-pieh Mountains. *Quat. Sci.* **2019**, *39*, 469–482.
- Jiang, F.; Xu, Q.; Zhang, S.; Li, F.; Zhang, K.; Wang, M.; Shen, W.; Sun, Y.; Zhou, Z. Relative pollen productivities of the major plant taxa of subtropical evergreen–deciduous mixed woodland in China. *J. Quat. Sci.* **2020**, *35*, 526–538. [[CrossRef](#)]

22. Wan, Q.; Zhang, Y.; Huang, K.; Sun, Q.; Zhang, X.; Gaillard, M.-J.; Xu, Q.; Li, F.; Zheng, Z. Evaluating quantitative pollen representation of vegetation in the tropics: A case study on the Hainan Island, tropical China. *Ecol. Indic.* **2020**, *114*, 106297. [[CrossRef](#)]
23. Wu, Z.Y. *Vegetation of China*; Science Press: Beijing, China, 1980.
24. He, Z.; Wu, Q.; Li, Y. Evaluation and Exploitation of the Meteorological Tourism Resources in Jinggangshan. *Jiangxi Sci.* **2018**, *36*, 262–296.
25. Huang, K.; Zheng, Z.; Liao, W.; Cao, L.; Zheng, Y.; Zhang, H.; Zhu, G.; Zhang, Z.; Cheddadi, R. Reconstructing late Holocene vegetation and fire histories in monsoonal region of southeastern China. *Palaeogeogr. Palaeoclimatol. Palaeoecol.* **2014**, *393*, 102–110. [[CrossRef](#)]
26. Liao, W.; Wang, Y.; Li, Z.; Peng, S.; Chen, C.; Fan, Q.; Jia, F.; Wang, L.; Liu, W.; Yin, G.; et al. *Intergrated Study on Biodiversity of Mount Jinggangshan Regions in China*; Science Press: Beijing, China, 2014.
27. Bunting, M.J.; Farrell, M.; Broström, A.; Hjelle, K.L.; Mazier, F.; Middleton, R.; Nielsen, A.B.; Rushton, E.; Shaw, H.; Twiddle, C.L. Palynological perspectives on vegetation survey: A critical step for model-based reconstruction of Quaternary land cover. *Quat. Sci. Rev.* **2013**, *82*, 41–55. [[CrossRef](#)]
28. Fægri, K.; Iversen, J. *Textbook of Pollen Analysis*; Wiley: New York, NY, USA, 1989.
29. Institute of Botany and South China Institute of Botany, A.S. *Angiosperm Pollen Flora of Tropic and Subtropic China*; Science Press: Beijing, China, 1982.
30. Wang, F.; Chien, N.; Zhang, Y.; Yang, H. *Pollen Flora of China*; Science Press: Beijing, China, 1995.
31. Tang, L.; Mao, L.; Shu, J.; Li, C.; Shen, C.; Zhou, Z. *An Illustrated Handbook of Quaternary Pollen and Spores in China*; Science Press: Beijing, China, 2016.
32. Gregory, P.H. *The Microbiology of the Atmosphere*; Leonard Hill: Aylesbury, UK, 1973.
33. Gaillard, M.-J.; Sugita, S.; Bunting, M.J.; Middleton, R.; Broström, A.; Caseldine, C.; Giesecke, T.; Hellman, S.E.V.; Hicks, S.; Hjelle, K.; et al. The use of modelling and simulation approach in reconstructing past landscapes from fossil pollen data: A review and results from the POLLANDCAL network. *Veg. Hist. Archaeobotany* **2008**, *17*, 419–443. [[CrossRef](#)]
34. Chaput, M.A.; Gajewski, K. Relative pollen productivity estimates and changes in Holocene vegetation cover in the deciduous forest of southeastern Quebec, Canada. *Botany* **2018**, *96*, 299–317. [[CrossRef](#)]
35. Abraham, V.; Kozáková, R. Relative pollen productivity estimates in the modern agricultural landscape of Central Bohemia (Czech Republic). *Rev. Palaeobot. Palynol.* **2012**, *179*, 1–12. [[CrossRef](#)]
36. Prentice, I.C. Pollen representation, source area, and basin size: Toward a unified theory of pollen analysis. *Quat. Res.* **1985**, *23*, 76–86. [[CrossRef](#)]
37. Kuparinen, A.; Markkanen, T.; Riikonen, H.; Vesala, T. Modeling air-mediated dispersal of spores, pollen and seeds in forested areas. *Ecol. Model.* **2007**, *208*, 177–188. [[CrossRef](#)]
38. Mariani, M.; Connor, S.E.; Theuerkauf, M.; Kuneš, P.; Fletcher, M.S. Testing quantitative pollen dispersal models in animal-pollinated vegetation mosaics: An example from temperate Tasmania, Australia. *Quat. Sci. Rev.* **2016**, *154*, 214–225. [[CrossRef](#)]
39. Li, F.; Gaillard, M.-J.; Xu, Q.; Bunting, M.J.; Li, Y.; Li, J.; Mu, H.; Lu, J.; Zhang, P.; Zhang, S.; et al. A Review of Relative Pollen Productivity Estimates From Temperate China for Pollen-Based Quantitative Reconstruction of Past Plant Cover. *Front. Plant Sci.* **2018**, *9*, 1214. [[CrossRef](#)]
40. Räsänen, S.; Suutari, H.; Nielsen, A.B. A step further towards quantitative reconstruction of past vegetation in Fennoscandian boreal forests: Pollen productivity estimates for six dominant taxa. *Rev. Palaeobot. Palynol.* **2007**, *146*, 208–220. [[CrossRef](#)]
41. Fang, Y.; Bunting, M.J.; Ma, C.; Yang, X. Are modern pollen assemblages from soils and mosses the same? A comparison of natural pollen traps from subtropical China. *Catena* **2022**, *209*, 105790. [[CrossRef](#)]
42. Theuerkauf, M.; Couwenberg, J. Pollen productivity estimates strongly depend on assumed pollen dispersal II: Extending the ERV model. *Holocene* **2021**, *32*, 1233–1250. [[CrossRef](#)]
43. Mazier, F.; Broström, A.; Gaillard, M.-J.; Sugita, S.; Vittoz, P.; Buttler, A. Pollen productivity estimates and relevant source area of pollen for selected plant taxa in a pasture woodland landscape of the Jura Mountains (Switzerland). *Veg. Hist. Archaeobotany* **2008**, *17*, 479–495. [[CrossRef](#)]
44. Wan, Q.; Zhang, X.; Huang, K.; Zheng, H.; Zhang, Y.; Yang, X.; Zheng, Z. Validation of relative pollen productivities for major tropical plant taxa: An empirical test using the REVEALS model in Hainan, China. *Quat. Int.* **2022**, *641*, 106–114. [[CrossRef](#)]

Disclaimer/Publisher’s Note: The statements, opinions and data contained in all publications are solely those of the individual author(s) and contributor(s) and not of MDPI and/or the editor(s). MDPI and/or the editor(s) disclaim responsibility for any injury to people or property resulting from any ideas, methods, instructions or products referred to in the content.